

Integrating Network Pharmacology and Component Analysis to Study the Potential Mechanisms of Qi-Fu-Yin Decoction in Treating Alzheimer's Disease

Xia Lei^{1,*}, Hongdan Xu^{2,*}, Yan Wang³, Hainan Gao⁴, Deping Zhao⁴, Jinfeng Zhang⁴, Ziyue Zhu⁴, Kun Zuo⁴, Ying Liu³, Xiaoliang Li^{3,5}, Ning Zhang⁴

¹Jiangsu CM Clinical Innovation Center of Degenerative Bone & Joint Disease, Wuxi TCM Hospital Affiliated to Nanjing University of Chinese Medicine, Wuxi, 214071, People's Republic of China; ²Department of Pharmacy, Wuxi Higher Health Vocational Technology School, Wuxi, 214000, People's Republic of China; ³Key Laboratory of Tropical Translational Medicine of Ministry of Education, Hainan Provincial Key Laboratory for Research and Development of Tropical Herbs, Haikou Key Laboratory of Li Nationality Medicine, School of Pharmacy, Hainan Medical University, Haikou, 571199, People's Republic of China; ⁴College of Pharmacy, Heilongjiang University of Chinese Medicine, Harbin, 150040, People's Republic of China; ⁵Key Laboratory of Tropical Cardiovascular Diseases Research of Hainan Province, Cardiovascular Diseases Institute of the First Affiliated Hospital, Hainan Medical University, Haikou, 571199, People's Republic of China

*These authors contributed equally to this work

Correspondence: Ning Zhang, College of Pharmacy, Heilongjiang University of Chinese Medicine, No. 24, Heping Road, Xiangfang District, Harbin, Heilongjiang Province, 150040, People's Republic of China, Email zhangning0454@163.com; Xiaoliang Li, College of Pharmacy, Hainan Medical University, No. 3 Xueyuan Road, Longhua District, Haikou City, Hainan Province, 571199, People's Republic of China, Email lixiaoliang-1984@163.com

Purpose: To elucidate the potential mechanisms of QFY for the treatment of Alzheimer's Disease (AD), and explore the effective substances of QFY.

Materials and Methods: UPLC-LTQ-Orbitrap-MS was used to identify the chemical constituents of the serum samples and the cerebrospinal fluid samples of rats after QFY administration. Network pharmacology was used to predict potential targets and pathways of QFY against AD. The AD mice model was established by subcutaneous injection of D-gal for 8 consecutive weeks. New object recognition (NOR) and Morris water maze test (MWM) were used to evaluate the learning and memory abilities of mice. Moreover, the levels of TNF- α , IL-1 β , and IL-18 in the brain hippocampus of mice were determined by ELISA. The expression of Bax, Bcl-2, Caspase-1, PSD95, SYP, ICAM-1 and MCP-1 proteins in the hippocampus was detected by Western blotting. Furthermore, qRT-PCR was used to detect the gene expressions of PSD95, SYP, M1 and M2 polarization markers of microglia, including iNOS, CD16, ARG-1, and IL-10 in the hippocampus.

Results: A total of 51 prototype compounds were detected in rat serum and 15 prototype components were identified in rat cerebrospinal fluid. Behavioral experiments revealed that QFY significantly increased the recognition index, decreased the escape latency, increased the platform crossing times and increased the residence time in the target quadrant. QFY also could alleviate the ultrastructural pathological changes in the hippocampus of AD mice. Meanwhile, QFY treatment suppressed the expression of inflammatory factors, such as TNF- α , IL-1 β , and IL-18. QFY improved the synaptic plasticity of the hippocampus in D-gal model mice by significantly increasing the expression of proteins and mRNAs of PSD95 and SYP.

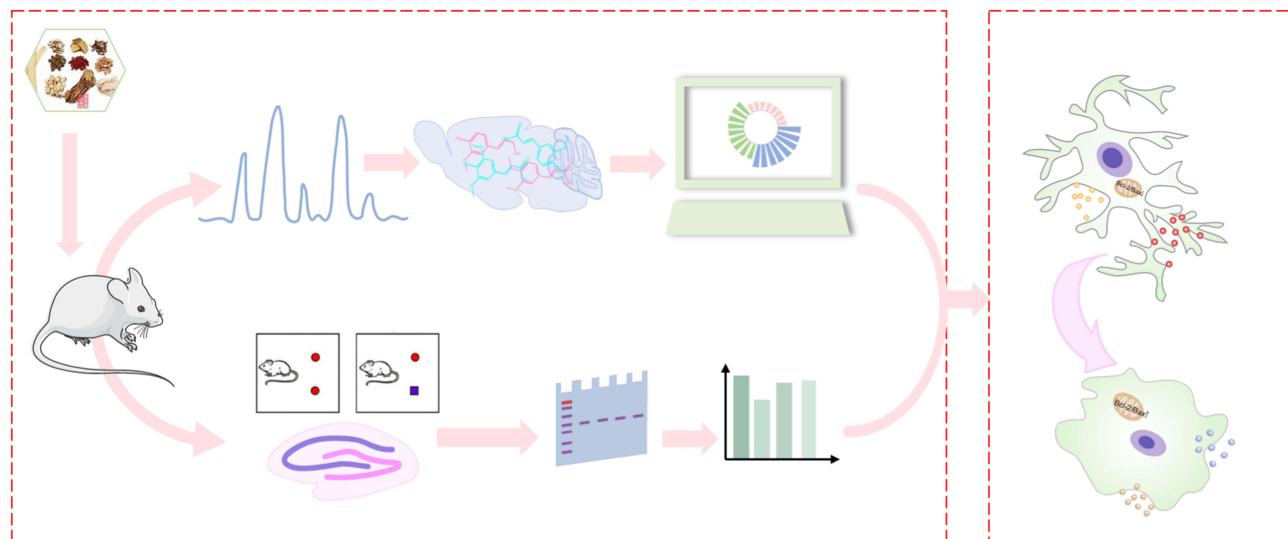
Conclusion: QFY could effectively improve the learning and memory impairment of D-gal-induced AD mice by inhibiting the excessive activation of microglia, enhancing the expression of M2 microglia, inhibiting the increase of inflammatory factors, cell adhesion factors and chemokines, anti-apoptosis, and improving synaptic plasticity.

Keywords: Qi-Fu-Yin, Alzheimer's disease, D-galactose, microglia phenotype, neuroinflammation

Introduction

AD is a neurodegenerative disease associated with aging, and its clinical manifestations are mainly cognitive dysfunction,¹ behavioral and psychological symptoms, and impairment of daily living functions.^{2,3} With the aging of the population in the world, AD has not only become a killer disease that threatens the health and even lives of the elderly,⁴ but also brings a huge

Graphical Abstract



social and economic burden. However, the pathogenesis of AD is complex, and clinical treatment with drugs, at present, is principally limited to symptomatic treatment,⁵ which cannot fundamentally prevent or reverse the process of the disease. Therefore, the search for drugs to prevent and delay the progress of AD or improve the symptoms of AD has become one of the most urgent tasks in the medical world.

TCM has a long history of preventing and treating AD, which is safe and effective.⁶ Especially in recent years, TCM has made good progress.⁷ QFY is a Ming Dynasty prescription recorded in *Jingyue Quanshu* compiled by Zhang Jingyue, which is composed of seven commonly used Chinese herbs,⁸ including: the radix of *Panax ginseng* C. A. Meyer (Araliaceae), the prepared rhizome of *Rehmannia glutinosa* (Gaetn.) Libosch. ex Fisch. et Mey. (Scrophulariaceae), the radix of *Angelica sinensis* (Oliv.) Diels (Umbelliferae), the rhizome of *Atractylodes macrocephala* Koidz (Asteraceae), the radix and rhizome of *Glycyrrhiza uralensis* Fisch. (Leguminosae), the seed of *Ziziphus jujuba* Mill.var.spinosa (Bunge) Hu ex H.F.Chou (Rhamnaceae), and the radix of *Polygala tenuifolia* Willd. (Polygalaceae).^{9,10} QFY, as a classic prescription for the treatment of AD, has also been reported clinically in recent years.¹¹ However, due to the lack of basic research, especially the mechanism of action of QFY in the treatment of AD is still unclear, it is difficult to further promote its application.

TCM formula is a complex system with multiple types of components, of which the active components can exert an integral effect by being absorbed into the blood and acting on the corresponding targets.¹² After the components of TCM enter the body, the interaction between the ingredients and the interaction between the ingredients and the body have added many obstacles to the research on the bioactive constituents of TCM.¹³ After gastrointestinal metabolism, the types and number of components in TCM are greatly reduced, thus simplifying the complexity of TCM research.¹⁴ Thus, the analysis of the components entering the blood and the brain can further clarify the bioactive constituents of TCM and its integrative mechanism. In the current study, the components of QFY entering the blood circulation and penetrating the blood brain barrier were analyzed using UPLC-LTQ-Orbitrap-MS. The mechanism of QFY improving neuroinflammation in an AD model mice induced by D-galactose was studied through behavioral, morphological, and molecular biological techniques. The findings obtained in the present study will lay a solid foundation for a wider and more reasonable clinical application of QFY in the treatment of AD.

Materials and Methods

Animals

Male Sprague-Dawley (SD) rats weighting 210–250 g (License No. SCXK-HEI- 2018-004) were provided by the experimental animal center of Heilongjiang University of Chinese Medicine. Male Kunming mice weighting 25–30 g (License No. SCXK-LIAO-2018-0001) were purchased from Liaoning Changsheng Biotechnology Co., Ltd (Shenyang, China). All animals were kept in a 12-hour light / dark cycle room with a humidity of 62±2% and a temperature of 21±2 °C. Animal experimentations were approved by the Ethics Committee of Heilongjiang University of Chinese Medicine (Approval No. 2020062202), and all animal procedures were conducted to follow the Regulations for the Administration of Affairs Concerning Experimental Animals approved by the State Council of the People's Republic of China.

Chemicals and Reagents

All herbs were purchased from Beijing Tongrentang Co., Ltd. (Beijing, China) and were authenticated by Xiaozhong Chen, associate professor of Heilongjiang University of Chinese medicine. D-galactose was purchased from Shanghai Macklin Biochemical Co., Ltd. Piracetam was purchased from Tianjin Jinshi Pharmaceutical Co., Ltd; The primary antibodies for Bcl-2, Caspase-1, Bax, PSD95, SYP and β -actin were purchased from Wuhan Boster Biological Technology Co., Ltd. IL-1 β , IL-18 and TNF- α ELISA kits were obtained from Elabscience Biotechnology Co., Ltd. DAPI purchased from Beijing Solarbio Science & Technology Co., Ltd.

Preparation of QFY Samples

Ginseng, prepared rehmannia root, Angelica sinensis, fried *Atractylodes macrocephala* Koidz, honey-fried licorice root, semen ziziphi spinosae and Processed Radix Polygalae were mixed according to the prescription ratio of QFY at 6:9:9:5:3:6:5. Then, the mixed herbal products were crushed into small pieces and decocted with 10 times the amount of water for 2 hours. The residue was decocted in the same amount of water for another hour. Subsequently, the filtrate was combined and condensed into 1g/mL liquid, which was stored in the refrigerator for later use.

Preparation of Rat Serum and Cerebrospinal Fluid Samples

SD rats were randomly divided into two groups, blank group and administration group, with 6 rats in each group. Distilled water and QFY liquid (7.74 g/kg) were given by gavage respectively. After administration, blood was collected from the orbits of rats at 30, 60, and 120 min respectively, centrifuged at 2000 rpm for 10 min, and the serum samples were stored at -80 °C. After blood collection, the rat head was fixed, and then cerebrospinal fluid was extracted with infusion needle and centrifuged at 2000rpm for 10min. The upper cerebrospinal fluid was collected and stored at -80°C.

UPLC-LTQ-Orbitrap-MS Analysis Conditions

The serum and cerebrospinal fluid samples analysis was performed using UPLC-LTQ-Orbitrap-MS. The samples were loaded onto an ACQUITY UPLC HSS T3 (100mm×2.1mm, 1.8 μ m) chromatographic columns at 40 °C. The mobile phase consisted of 0.1% formic acid-water (A) and 0.1% formic acid-acetonitrile (B). The flow rate was 0.4 mL/min, and the gradient elution program was as follows: 0–3.5 min: 0–15% B; 3.5–6 min: 15–30% B; 6–12 min: 30–70% B; 12–12.5 min: 70% B; 12.5–18 min: 70–100% B; and 18–24 min: 100% B. The injection volume was 5 μ L.

The mass spectrometer system equipped with an electrospray ionization source, and the spray voltages in positive and negative ion modes were set to 3.5 KV and 3.2 KV, respectively. The temperature of ion transfer tube was maintained at 320 °C and the auxiliary gas heating temperature was set at 350 °C. Full scans of 50 to 1500 m/z were subjected in the Orbitrap mass spectrometers.

Network Pharmacology Analysis

The chemical composition information from QFY absorbed into brain were collected from Traditional Chinese Medicine Systems Pharmacology (TCMSP, <http://tcmspw.com/>) and DrugBank (<https://drugbank.ca/>). The potential targets of the components were supplemented through the Swiss Target Prediction website (<http://www.swisstargetprediction.ch/>). All targets

related to AD were determined by DisGeNET (<https://www.disgenet.org/>). The protein-protein interaction (PPI) network was visualized by Cytoscape (Version 3.8.2) software. Metascape (<http://metascape.org/gp/index.html#/main/step1>) was used for GO functional annotation and KEGG pathway analysis.

Animal Grouping and Treatments

After 1 week of acclimation, the mice were randomly assigned to four groups: (1) normal control group (n=15), (2) D-gal group (125mg/kg/d, n=15), (3) D-gal plus piracetam treatment (208mg/kg/d, n=15), and (4) D-gal plus QFY treatment (11.18g/kg/d, n=15). Mice in each administration group and D-gal group were subcutaneously injected with D-gal for 8 consecutive weeks, while normal control group was given the same dose of normal saline. Except that the normal control group and D-gal group were given the same dose of normal saline, the other groups were administered corresponding drugs by gavage.

Behavioral Analysis

Novel Object Recognition (NOR) Test

In the NOR, all mice were individually exposed to an empty arena for 5 min without limitation during the environment habituation period. The next day, the mice were placed in the arena with their backs facing two identical objects for 5 min. After an hour's interval, one of the two same objects was exchanged for a different one, and then the mice were put back into the arena again for 5 min. The contact time of the mice to the novel object (TN) and the contact time of the mice to the familiar object (TF) within 5 min were recorded separately. The recognition index (RI), which reflects the learning and memory abilities of mice to explore novel objects, was defined as $RI = (Tn - Tf) / (Tn + Tf)$.

Morris Water Maze (MWM) Test

The circular pool was divided into 4 quadrants, and a platform was placed in the fourth quadrant and submerged 2cm below the water surface. In the first 4 days, animals in each group were placed in the maze facing the pool wall in quadrants 1, 2, and 3, respectively. The mice were given 90s to find the platform and allowed to stay on it for 30s. Mice that failed to find the submerged platform within 90s were directed onto the platform and remained there for 30s, and the escape latency was recorded as 60s. On day 5, the submerged platform was removed in the probe trial. The number of times the mice crossed the previous position of the platform and the residence time in the target quadrant within 90s were recorded and analyzed.

Histopathologic Examinations

Hematoxylin-Eosin (HE) Staining

After fixation with 4% paraformaldehyde, the brain tissues of mice were dehydrated, embedded in paraffin, sectioned, dewaxed, stained with hematoxylin, and sealed with neutral gum. The histopathological changes were observed under light microscope.

Immunofluorescence Staining

The expression level of Iba-1 in brain tissues of mice was detected by immunofluorescence staining. Tissue sections were blocked in 5% BSA for 1 h followed by incubation with the primary antibodies at 4 °C overnight. After being washed, the sections incubated with the secondary antibody for 1 h at room temperature. Finally, the nucleus was stained with DAPI for 5 min. The sections were imaged under a confocal microscope.

Transmission Electron Microscope (TEM)

The hippocampus of mice was immersed in 2.5% glutaraldehyde at 4 °C for 4 h and then transferred to 1% osmic acid for fixation. The samples were gradient dehydrated, embedded with epoxy resin and cut into 70–90 nm. The sections were stained with 2% toluidine blue and observed under the TEM.

Enzyme-Linked Immunosorbent Assay (ELISA)

The levels of inflammatory factors TNF- α , IL-1 β and IL-18 were detected in the hippocampus of mice according to the instructions of ELISA kit. Specifically, 50 μ L of blank, standard, and sample solutions were added to the 96 well plate supplied in the reagent kit. Following 30 minutes of incubation at 37 °C, the 96 well plate was washed using buffer solution. With the exception of blank wells, each well was added with 100ul of enzyme-labeled reagent, incubated, and then added with chromogenic agent. After the reaction was terminated, the absorbance was measured at 450nm.

Western Blot Analysis

The total protein of hippocampus in mice was extracted and quantified with BCA protein assay kit. Samples were separated by 10% SDS-PAGE gel and then transferred to the PVDF membrane. After blocking the membrane with 5% skim milk for 2 h, the primary antibody was added and incubated at 4 °C overnight. The primary antibodies used were as follows: PSD95, SYP, Bax, Bcl-2, Caspase-1, ICAM-1 and MCP-1. The blots were incubated with HRP-conjugated secondary antibody (1:5000) for 2 h. Finally, Lane 1D software of gel imaging system was used for detection.

RT-PCR Assay

Total RNA samples from the hippocampus in mice were extracted via the TRIzol reagent according to the manufacturer's protocols, and then the concentration of RNA was measured by Nanodrop 2000. The relative expression of the target mRNA was normalized with β -actin using the $2^{-\Delta\Delta C_t}$ method. The primer sequences are shown in [Table 1](#).

Statistical Analysis

All results were expressed as mean \pm SD and analyzed by SPSS 21.0 software. The Shapiro–Wilk test and Q-Q plots were utilized to determine whether the data conformed to a normal distribution. The two-sample *t*-test was utilized for the comparison of the two groups, while statistical evaluations among multiple groups were determined by a one-way ANOVA followed by post-hoc tests. A value of $P < 0.05$ was considered statistical significance.

Results

Identification Constituents of QFY in Rat Serum and Cerebrospinal Fluid

To accurately analyze the effective compounds in QFY, the UPLC-LTQ-Orbitrap-MS method was used to detect the components of QFY in rat serum and cerebrospinal fluid in the positive and negative ion modes, respectively. The total ion chromatograms were shown in [Figure 1](#). According to retention time, mass-to-charge ratio, fragmentation behavior and related database, a total of 51 prototype compounds were detected in rat serum and 15 prototype components were identified in rat cerebrospinal fluid after the oral administration of QFY. Surprisingly, the 15 prototype components found in cerebrospinal fluids were also components in blood. Detailed information for each constituent was listed in [Table 2](#). The structural formula of QFY components entering into blood and brain were shown in [Supplementary Figure 1](#).

Table 1 Primer Sequence of Target Gene and Internal Reference Gene

Primer Name	Upstream Primer (5'-3')	Downstream Primer (3'-5')
PSD95	CCATCGCCATCTTCATCCG	CATCTCCCGCTGTCGAACTTC
SYP	TGTTTGCCTTCTACTCCATG	TACTACCTGAAAGACCGATGTCG
iNOS	AATGCCCGTACCAGGCCAAT	GGTCACCTACCGCACCCGAGAT
CD16	ACTGTGGTTGGCTTTTGGGAT	GAGTGATTTCTGACTGGCTGCTG
Arg-1	TCTTTGGCAGATATGCAGGGA	CACAGTCTGGCAGTTGGAAGC
IL-10	GCCTGGGGCATCACTTCTACC	CTGGACAACATACTGCTAACCGAC
β -actin	GGCTGTATCCCCCTCCATCG	TGTACCGTAACAATGGTTGACC

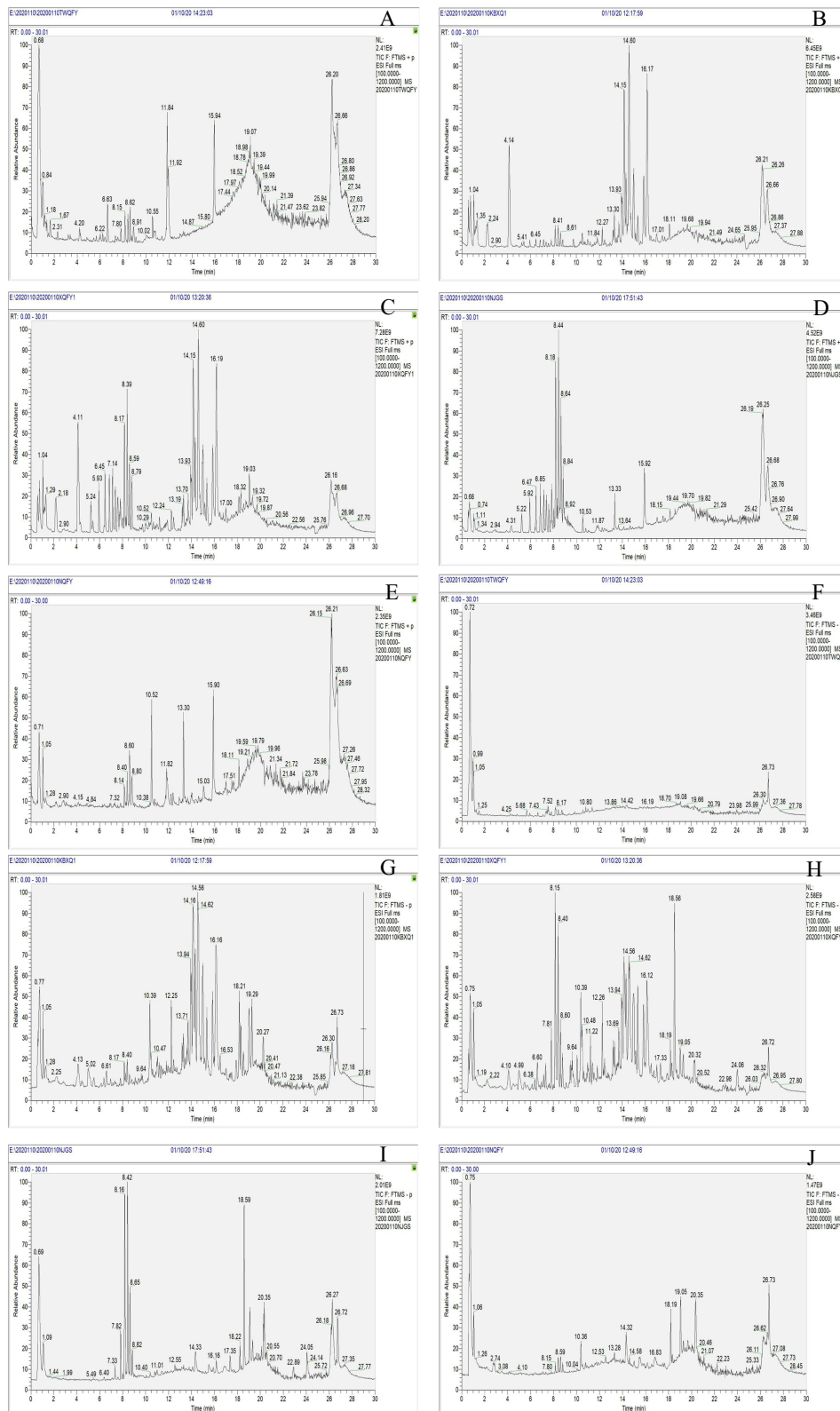


Figure 1 Total ion chromatograms of QFY in rat serum and cerebrospinal fluid were determined by UPLC-LTQ-Orbitrap-MS. Positive ion mode: (A) QFY sample, (B) blank serum, (C) serum containing QFY, (D) blank cerebrospinal fluid and (E) cerebrospinal fluid containing QFY. Negative ion mode: (F) QFY sample, (G) blank serum, (H) serum containing QFY, (I) blank cerebrospinal fluid and (J) cerebrospinal fluid containing QFY.

Table 2 Identification of Phytochemical Constituents of QFY in Rat Serum and Cerebrospinal Fluid

NO.	t _R (Min)	Formula	Molecular Weight	Ionization Mode	Fragment Ions (m/z)	Identification
1	0.77	C18H32O16	549.16617	[M-H] ⁻	383.12, 341.11, 101.02, 89.02, 59.02	Mannotriose
2	3.65	C16H22O10	373.11319	[M-H] ⁻	149.06, 123.04	Geniposide acid
3	4.44	C16H18O9	353.08724	[M-H] ⁻	191.05, 179.03, 135.04	Neochlorogenic acid
4	4.7	C16H24O10	375.12895	[M-H] ⁻	213.08, 169.09, 151.02, 95.05, 59.01	Loganic acid
5	4.95	C16H17NO3	272.12732	[M+H] ⁺	161.06, 107.05	Higenamine
6*	5.29	C10H12O3	163.07499	[M+H] ⁺	131.05, 107.05, 103.05	Coniferyl alcohol
7	5.63	C16H18O9	353.08713	[M-H] ⁻	353.08, 191.05	Chlorogenic acid
8	5.81	C22H30O14	517.15505	[M-H] ⁻	175.04, 160.02	Sibiricose A5
9	6.07	C23H32O15	547.16581	[M-H] ⁻	223.06, 205.05, 190.03, 175.00	Sibiricose A6
10	6.32	C18H19NO4	312.12349	[M-H] ⁻	297.10, 282.08, 284.08	Lauroilsine
11*	6.63	C19H21NO4	328.15346	[M+H] ⁺	297.11, 265.09	Boldine
12	6.67	C27H30O15	593.15042	[M-H] ⁻	353.07, 297.08	Vicenin II
13	7.02	C17H20O9	367.1025	[M-H] ⁻	191.05, 173.04, 134.04, 93.03	3-O-Feruloylquinic acid
14	7.08	C26H28O14	563.13966	[M-H] ⁻	383.08, 353.07, 325.07, 297.08	Isoschaftoside
15	7.17	C24H26O14	537.12387	[M-H] ⁻	285.04, 267.03, 257.05	Sibiricaxanthone B
16	7.34	C27H30O15	593.1502	[M-H] ⁻	413.09, 293.05, 175.00	Vitexin-4''-O-glucoside
17	7.4	C25H28O15	567.13437	[M-H] ⁻	345.06, 297.04, 282.02, 272.03	Polygalaxanthone III
18	7.46	C24H34O15	607.18664	[M-H] ⁻	561.18, 323.10, 237.08, 103.05	Glomeratose A
19*	7.59	C11H12O4	191.06979	[M+H] ⁺	146.94, 145.86, 102.95, 87.92	3,4-Dimethoxycinnamic acid
20*	7.59	C15H12O4	257.08012	[M+H] ⁺	147.04, 137.02	Isoliquiritigenin
21	7.62	C21H22O9	419.13238	[M+H] ⁺	257.08, 147.04, 137.02	Isoliquiritin
22	7.69	C21H22O9	417.11837	[M-H] ⁻	255.07, 135.01	Liquiritin
23*	7.7	C10H10O4	177.05418	[M+H] ⁺	177.05, 134.04	Ferulic acid
24*	8.29	C11H12O5	207.06455	[M+H] ⁺	47.04, 119.05, 91.05	3,5-dimethoxy-4-hydroxycinnamic acid
25	8.36	C21H22O10	433.11303	[M-H] ⁻	356.97, 261.78, 123.04, 101.02	Naringenin-7-o-glucoside
26	8.62	C47H80O18	977.5299	[M-H] ⁻	931.52, 799.48, 475.38, 101.02, 71.01	Notoginsenoside R1
27	8.74	C27H30O13	607.16577	[M-H] ⁻	619.37, 361.64, 237.08, 161.02	Glycyroside
28	8.81	C12H14O5	221.08013	[M+H] ⁺	190.06, 147.04	3,4,5-Trimethoxycinnamic acid
29	8.82	C31H38O17	681.20203	[M-H] ⁻	443.12, 137.02	Tenuifoliside A
30	9.01	C16H12O4	269.08	[M+H] ⁺	237.05, 213.09, 118.04	Formononetin
31	9.01	C22H22O9	413.12189	[M+H] ⁺	147.04, 119.05, 105.03	Ononin
32	9.35	C16H14O5	285.07636	[M-H] ⁻	270.05, 177.02, 150.03, 49.02	Licochalcone B
33	9.58	C15H20O4	263.12821	[M-H] ⁻	219.14, 204.11, 151.07, 136.05	Abscisic acid
34*	10.6	C30H46O5	469.32983	[M+H] ⁺	189.16, 187.15, 175.15, 119.09	Quillaic acid
35*	10.63	C54H92O23	1131.58783	[M+H] ⁺	945.54, 783.49	Ginsenoside Rb1
36	10.63	C30H48O	407.36595	[M+H] ⁺	217.19, 147.12, 109.10, 95.09	Lupenone
37	10.85	C36H56O12	593.15031	[M-H] ⁻	455.32, 425.31, 71.01, 59.01	Tenuifolin
38*	10.86	C30H46O3	437.34008	[M+H] ⁺	187.15, 123.12, 121.10, 81.07	Wilforlide A
39	10.86	C30H48O4	455.35046	[M+H] ⁺	135.12, 131.22, 95.09	Corosolic acid
40	10.87	C48H76O19	955.48729	[M-H] ⁻	569.38	Ginsenoside Ro
41	10.93	C53H90O22	1123.58726	[M-H] ⁻	1077.58, 945.54, 191.05, 101.02	Ginsenoside Rc
42*	10.95	C53H90O22	1101.57807	[M+H] ⁺	789.47, 335.09	Ginsenoside Rb3
43	11.2	C15H12O4	255.0656	[M-H] ⁻	135.01, 119.05, 91.02	Liquiritigenin
44	11.34	C48H82O18	991.54597	[M-H] ⁻	783.49, 113.02, 101.02, 71.01	Ginsenoside Rd
45*	11.42	C42H62O16	823.4088	[M+H] ⁺	453.34, 121.10, 95.09	Glycyrrhizic acid
46*	12.85	C15H20O3	231.13737	[M+H] ⁺	167.46, 134.32, 99.92, 88.9	Atractylenolide III
47*	12.91	C12H16O2	193.12184	[M+H] ⁺	175.11, 147.12, 137.06, 105.07, 91.05	Senkyunolide A
48	13.07	C42H72O13	829.49405	[M-H] ⁻	621.43, 113.02, 101.02, 71.01	Ginsenoside Rg3
49	13.15	C21H22O4	339.15802	[M+H] ⁺	297.15, 121.03, 107.05	Licochalcone A
50*	13.82	C12H14O2	191.10611	[M+H] ⁺	145.10, 117.07, 91.05	Ligustilide
51*	14.2	C15H20O2	233.15293	[M+H] ⁺	233.15, 187.15, 131.08, 151.08	Atractylenolide II

Note: *Represents the shared components in the blood and brain.

Analysis of Candidate Targets of QFY Against AD

In order to explore the protective mechanism of QFY against AD, the potential targets of QFY in AD were analyzed by network pharmacology. As a result, there were 115 intersecting targets between ingredients of QFY absorbed into brain and AD (Figure 2A). PPI network analysis of 114 intersecting targets yielded 25 core target genes of QFY acting on AD. GO analysis showed that these genes were mainly related to protein kinase activity, cellular response to nitrogen compound and membrane raft, etc. (Figure 2D). As shown by the KEGG pathways (Figure 2E), the most related pathway mainly involved in Alzheimer's disease, HIF-1 signaling pathway, apoptosis, etc. Finally, we mapped QFY, 15 prototype components in rat cerebrospinal fluid and the predicted targets onto 20 corresponding pathways, as shown in Figure 2C.

QFY Attenuated Learning and Memory Impairment in D-Gal-Treated Mice

In the NOR memory test, the RI of the AD mice stimulated with D-gal decreased obviously ($P < 0.01$) compared with the control group. However, QFY group and piracetam group increased the RI significantly ($P < 0.01$) compared with model group, indicating that the administration of QFY improved D-gal-induced impairment of NOR memory in mice (Figure 3A).

In MWM, compared with the control group, mice in the D-gal model group exhibited longer escape latency to the platform, lower crossing times and residence time in the target quadrant, indicating that spatial learning and memory abilities of mice was impaired by D-gal induction. Whereas, QFY and piracetam significantly mitigated the above trend. The findings revealed that QFY could block memory impairment caused by D-gal and make the model mice to find the platform more easily and quickly (Figure 3B–D).

QFY Treatment Inhibited Hippocampal Neuronal Damage in D-Gal-Treated Mice

As shown in Figure 4A, pyramidal cell of hippocampal in the control group were normal in shape, with round cell bodies and clear nuclei and nucleoli. The D-gal-treated group exhibited atrophy and deformation of most cells, cellular karyopyknotic and an expanded gap of neurons. However, degenerative alterations and neuronal atrophy were obviously attenuated by QFY and piracetam administration. In addition, TEM revealed that the neurons in the control group were intact, with homogeneous nuclei, evenly distributed chromatin, normal mitochondrial structure, clear and intact bilayer structure of the cristal membrane, whereas after D-gal treatment, neurons in the hippocampus exhibited shrinking nuclei, blurred or vacuolated cristae of mitochondria, and uneven postsynaptic density. The ultrastructure of neurons in the QFY groups was obviously improved to varying degrees (Figure 4B). Collectively, these data visually indicated that QFY could effectively alleviate the injury of hippocampal neurons in AD mice induced by D-Gal.

Effect of QFY on the Expression Levels of PSD95 and SYP in D-Gal Model Mice

The mRNA and protein expression levels of PSD95 and SYP in the hippocampus of mice were significantly down-regulated in the model group compared with the control group. However, compared with the model group, those treated with QFY and piracetam exhibited the increased mRNA and protein expression of PSD95 and SYP in the hippocampus, respectively (Figure 5A and B).

QFY Suppressed D-Gal-Induced Apoptosis

As shown in Figure 5C, D-gal caused a significant increase in Bax and Caspase-1 and an obvious decrease in Bcl-2 in the hippocampus of mice compared with the control group. In contrast, these changes were obviously alleviated by QFY treatment.

Effect of QFY on Hippocampal Neuroinflammation in D-Gal Model Mice

QFY Attenuated the Activated Microglia

Free calcium binding adaptor molecule-1 (Iba-1) is widely used as a marker of microglia. In the D-gal model group, the expression of Iba-1 was significantly enhanced, and the number of activated MG was notably increased, while piracetam and QFY could effectively reduce the number of microglia and protect the hippocampus from inflammatory damage (Figure 6).

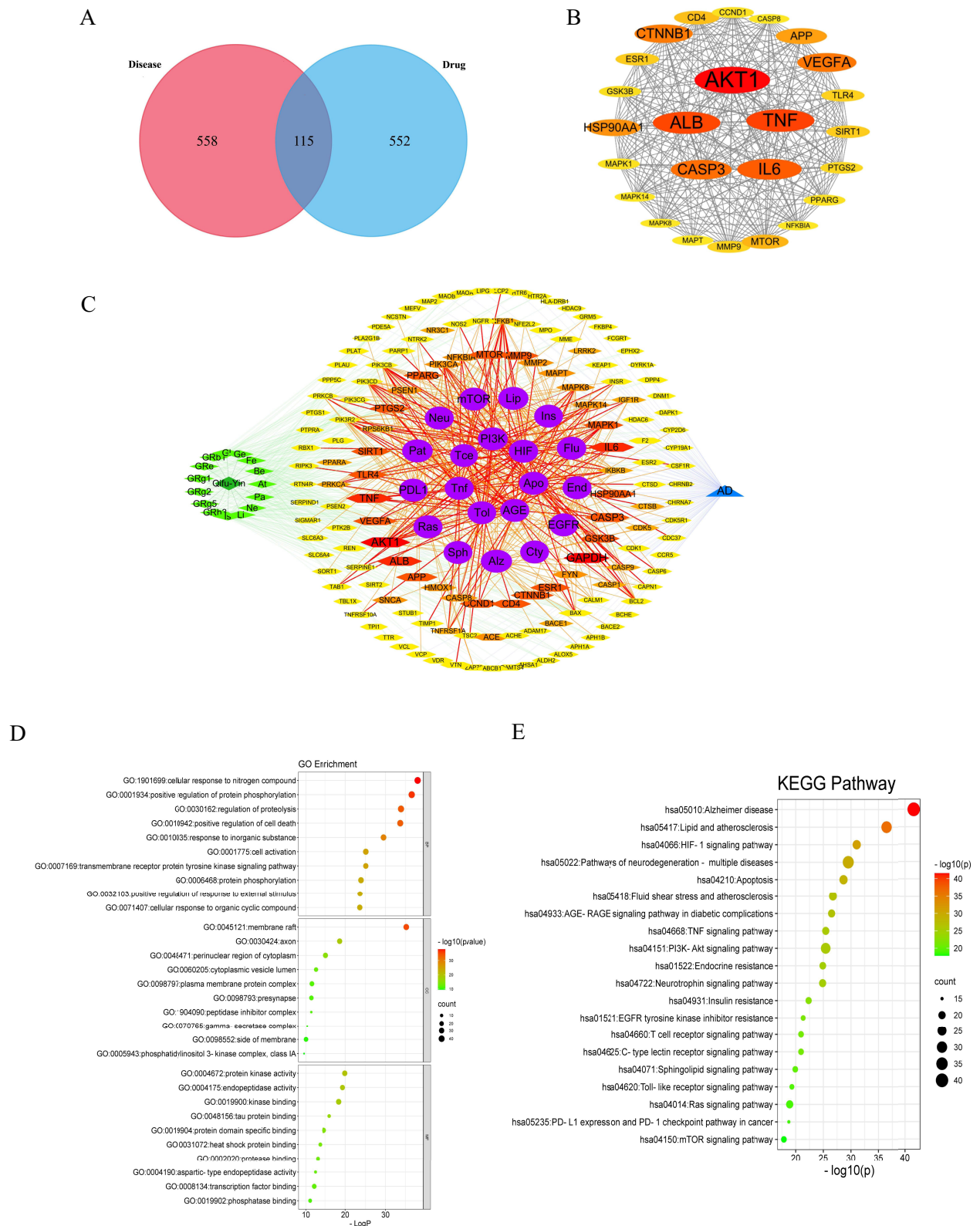


Figure 2 Network pharmacology analysis of ingredients of QFY absorbed into brain against AD. **(A)** Venn Diagram: the intersection of QFY targets and AD targets. **(B)** The core targets of QFY acting on AD. **(C)** Compound-target-pathway network of QFY for the treatment of AD. **(D)** GO function analysis. **(E)** KEGG pathway enrichment analysis.

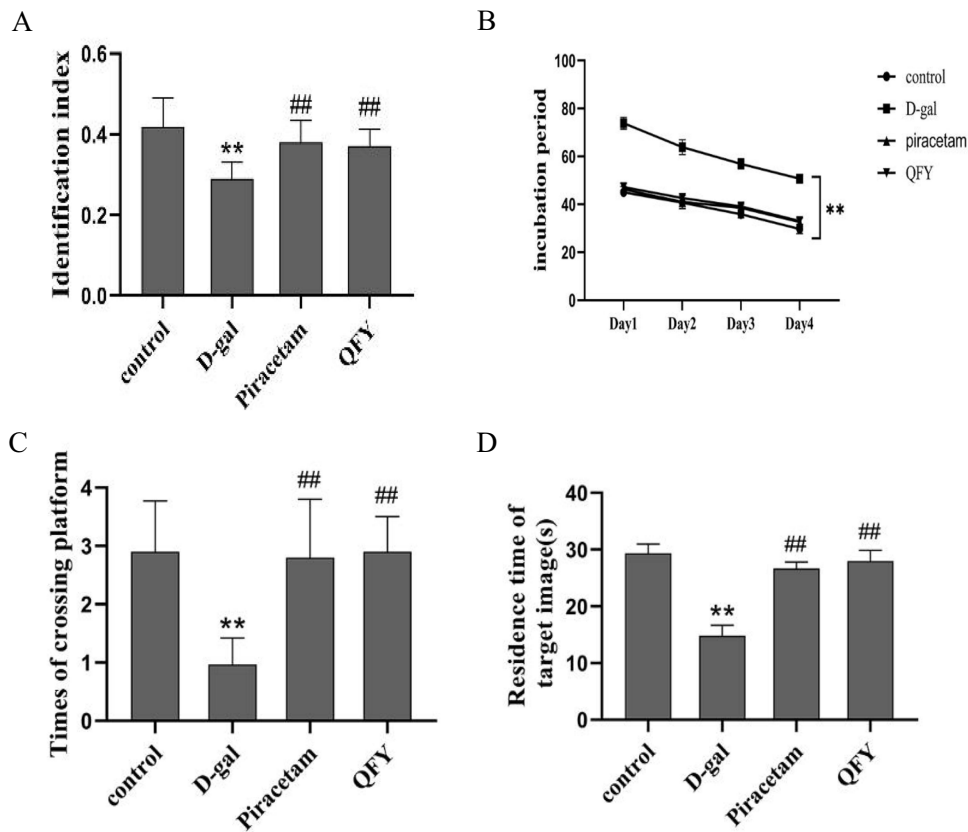


Figure 3 Effect of QFY on cognitive impairment caused by D-gal administration. (A) The RI of NOR. (B) The escape latency of MWM. (C) The number of times the mice crossed the platform. (D) the time spent in the target quadrant. n = 15 in each group, **P < 0.01 vs the control group; ##P < 0.01 vs the model group.

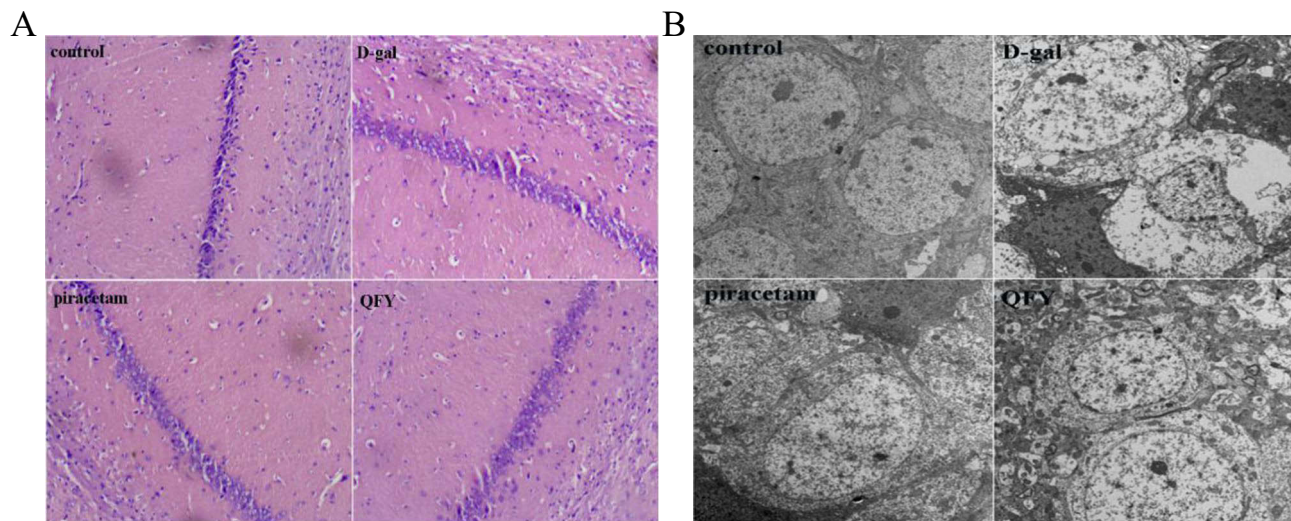


Figure 4 Effects of QFY on histopathological and ultrastructural alterations in the hippocampus of AD mice. (A) HE staining of mice hippocampus (×200, n = 15 in each group). (B) Ultrastructural observation of hippocampus in mice by TEM (×22,000, n = 15 in each group).

QFY Inhibited the Release of Inflammatory Cytokines

In addition, the changes of inflammatory cytokines, including IL-18, IL-1β and TNF-α, were detected in the hippocampus of D-gal model mice. The present experimental results showed that IL-18, IL-1β and TNF-α levels in the hippocampus of

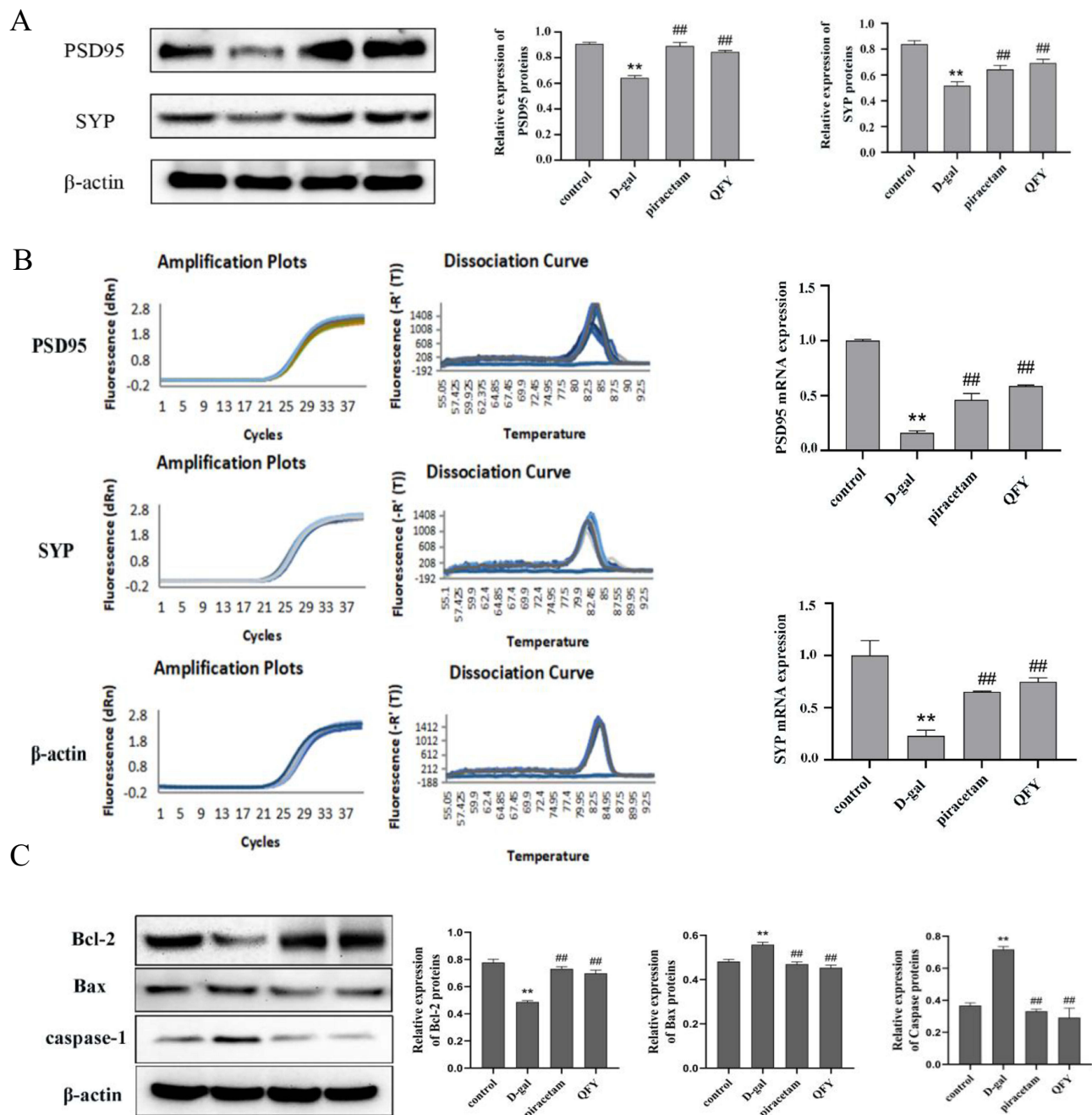


Figure 5 The effect of QFY on synapses and neuronal apoptosis. **(A)** The expression of PSD95 and SYP protein in mice hippocampus. **(B)** Amplification curve, fusion curve and mRNA expression of PSD95 and SYP. **(C)** The expression of Bax, Bcl-2, and Caspase-1 protein in mice hippocampus. $n = 5$ in each group, ** $P < 0.01$ vs the con group; ### $P < 0.01$ vs the model group.

D-gal model mice were remarkably decreased after QFY treatment, further supporting the theory that QFY may reduce neuroinflammation (Figure 7C).

QFY Regulated the Expression of Markers of M1 and M2 Microglia

Compared with the control group, the mRNA expression levels of M1 microglia markers including iNOS and CD16, and M2 microglia markers including Arg-1 and IL-10 were all significantly increased in the model group. However, the mRNA expression of iNOS, CD16, Arg-1 and IL-10 in piracetam group and QFY group was significantly lower than that in D-gal model group (Figure 7A).

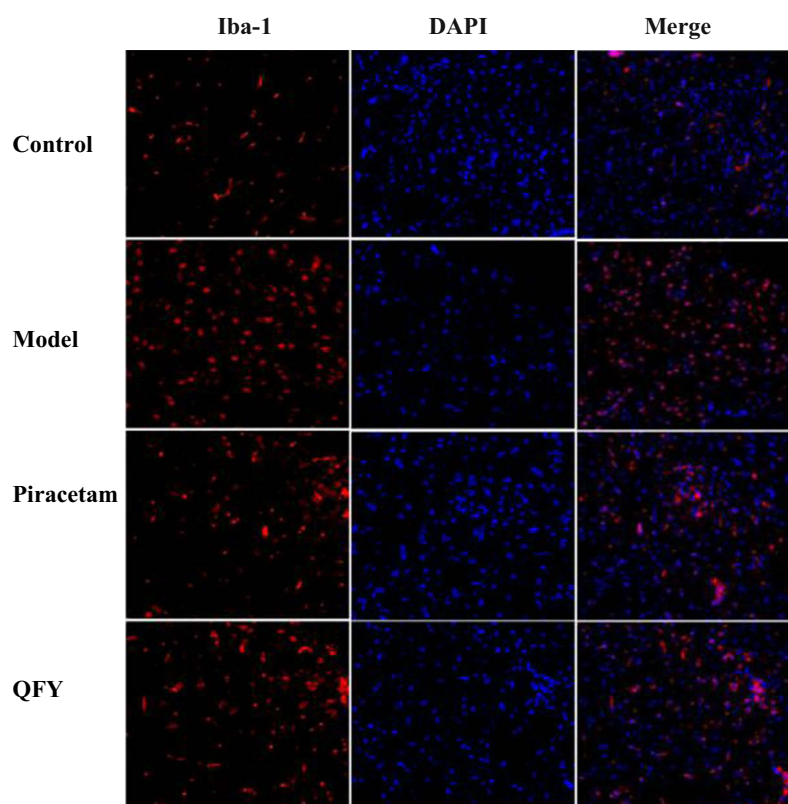


Figure 6 Immunofluorescence staining of Iba-1 ($\times 400$, $n = 15$ in each group).

QFY Regulated the Expression of ICAM-1 and MCP-1 Proteins

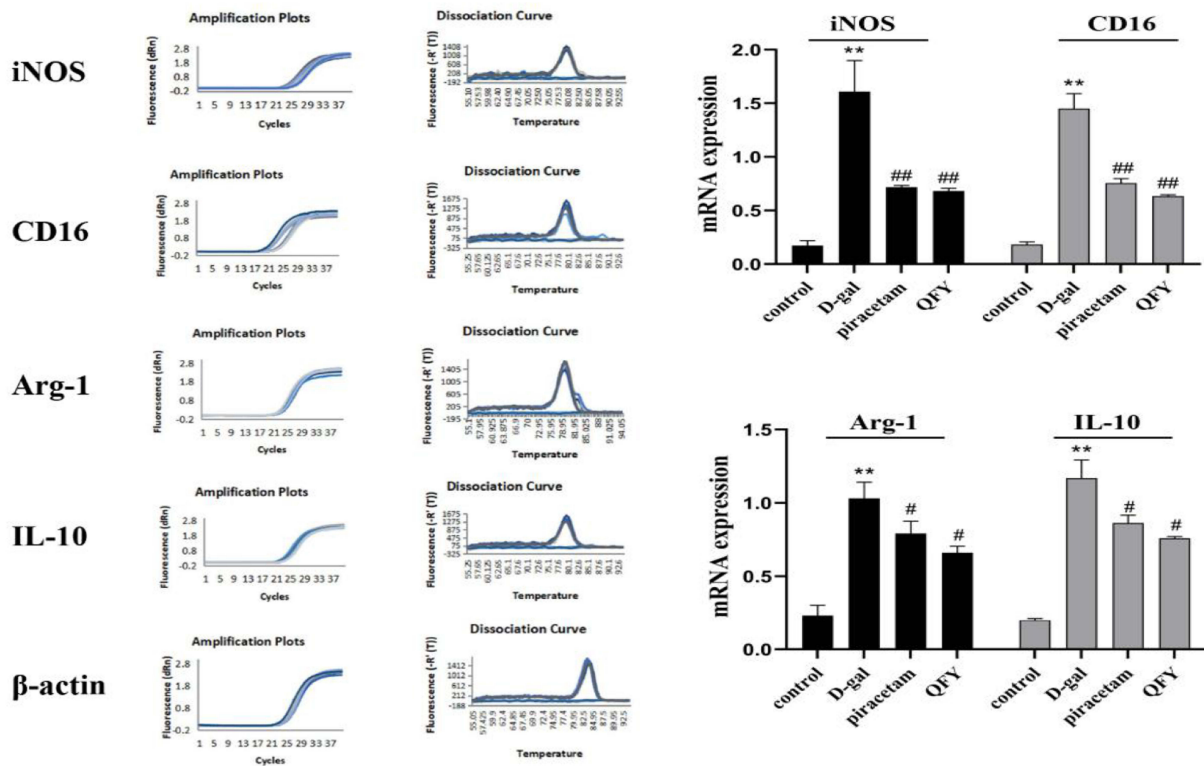
As shown in [Figure 7B](#), the expressions of ICAM-1 and MCP-1 proteins in the hippocampus were significantly increased in the D-gal model group compared with the control group, while the administration of piracetam and QFY obviously decreased the levels of ICAM-1 and MCP-1. These results indicated that QFY can not only reduce the release of inflammatory factors, but also inhibit the release of adhesion factors and chemokines, and synergistically resist neuroinflammation.

Discussion

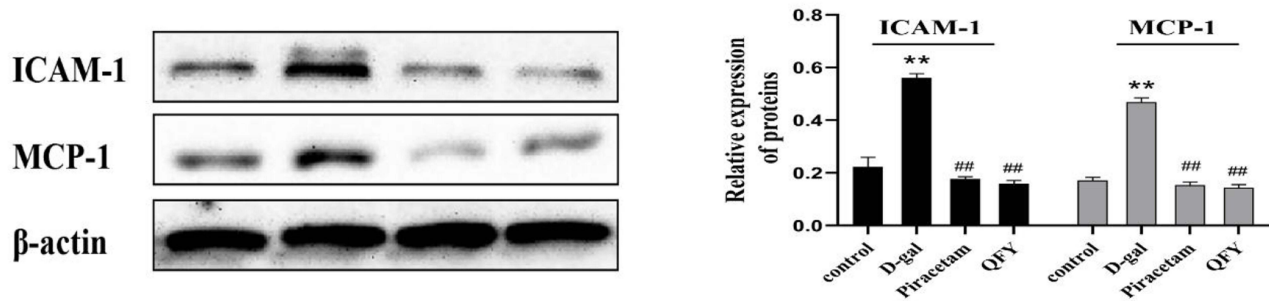
AD is a neurodegenerative disease with memory loss and cognitive dysfunction as the main clinical manifestations.¹⁵ Sadly, there is no ideal treatment so far. Although QFY, as a famous traditional Chinese medicine compound, has a good therapeutic effect on AD, its complex components and unclear mechanism of action limit its wide application. As we all know, components that are absorbed into the blood and reach a certain concentration are considered to be effective.^{16,17} Especially for central nervous system diseases, substances that can penetrate the blood-brain barrier may be the real material basis of traditional Chinese medicine compounds.¹⁸

The present study found that a total of 51 prototype compounds of QFY were detected in rat serum and 15 prototype components of QFY were identified in rat cerebrospinal fluid, including flavonoids, triterpenoid saponin, alkaloids, organic acids, etc. In recent years, more in-depth studies have been conducted on the oligosaccharide esters in *Polygala tenuifolia* Willd. The identified glomeratose A, sibiricose A5, and sibiricose A6 can significantly enhance the learning and memory abilities of mice, reduce the MDA content in the hippocampus, and ameliorate cognitive dysfunction in mice.¹⁹ Evidence suggests that Tenuifolin has a considerable anti-cholinesterase effect, and research conducted on dementia mice showed that it could improve their cognitive abilities, inhibit AchE activity, and promote ChAT activity and synaptic plasticity.²⁰ *Glycyrrhiza uralensis* Fisch. contains a variety of licorice flavonoids, including flavonoids, isoflavones, chalcones, and dihydroflavonoids, which are all considered to be active substances. Licochalcone A has been

A



B



C

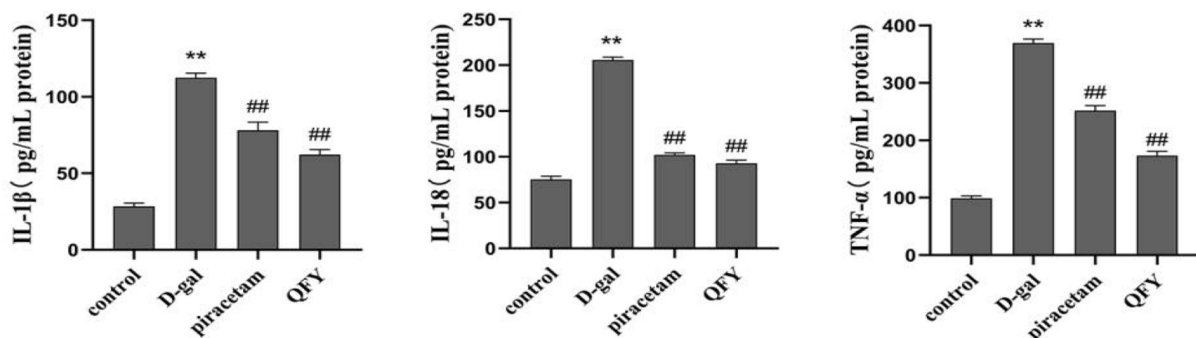


Figure 7 The effect of QFY on hippocampal neuroinflammation in mice. **(A)** M1 markers iNOS, CD16, M2 markers Arg-1, IL-10 mRNA expression. **(B)** Immunoblotting of ICAM-1 and MCP-1 proteins in the hippocampus of mice. **(C)** The contents of IL-1 β , IL-18, and TNF- α in the hippocampus of mice. n = 15 in each group, **P < 0.01 vs the con group; ##P < 0.01 vs the model group; #P < 0.05 vs the model group.

demonstrated to be effective in reducing inflammation, as it suppresses the production of toxins such as NO and the chemokine MCP-1.²¹ Isoliquiritigenin can inhibit the excessive reactive oxygen species produced by iron poisoning, reduce apoptosis and improve mitochondrial dysfunction.²² Liquiritin can enhance the expression of neurotrophic factor and improve learning and memory abilities to prevent and treat AD.²² Vicenin II and vitexin-4''-O-glucoside have flavonoid structures and are the main active substances of *Ziziphus jujuba* Mill.var.spinosa. The flavonoids from *Ziziphus jujuba* Mill.var.spinosa can obviously prolong the incubation period of mice, reduce the number of wrong reactions and shorten the time of electric shock, indicating that it can improve the learning and memory abilities of mice.²³ Ferulic acid in *Angelica sinensis* (Oliv.) Diels belongs to aromatic acid compounds. Sodium ferulic acid has been developed clinically, which can reduce cell damage in patients with cerebral infarction and improve their the memory abilities and cognitive function in those with AD.²⁴ Atractylenolide II and III belong to sesquiterpene lactones in structure and are the characteristic components of *Atractylodes macrocephala* Koidz. They can enhance the learning and memory abilities of dementia mice, increase the ACh level in the learning and memory functional area, and improve cognitive dysfunction.²⁵ Mannotriose is an active component of Chinese Foxglove, which can protect rat hippocampal neurons from damage caused by high concentrations of corticosterone,²⁶ and improve the degeneration of learning and memory function by regulating the expression of GCR, BDNF and SGK in the learning and memory signal transduction pathway.²⁷ The main active ingredient in *Panax ginseng* C. A. Mey. are ginsenosides, including oleanolane type (Ro), protopanaxadiol type (Rb1, Rb3, Rd, Rc, Rg3), protopanaxatriol type (notoginsenoside R1). Among them, ginsenoside Rb1 can effectively inhibit the toxicity of α -synuclein in the central nervous system and prevent neuronal degeneration.²⁸ Ginsenoside Rd maintains mitochondrial function by reducing oxidative stress damage and inhibiting apoptosis.²⁹ In addition, notoginsenoside R1 has the effects of anti-inflammatory, protecting the nervous system and scavenging oxygen free radicals. Chlorogenic acid is a polyphenolic compound, which has good effects in anti-inflammatory, antioxidant and protection of the nervous system.³⁰ It can reduce the production of some pro-inflammatory mediators, including TNF- α , IL-1 β and IL-6, and alleviate the inflammatory response of the central nervous system.³¹ Geniposidic acid, an iridoid compound, can improve the learning and memory abilities of dementia mice, inhibit the expression of inflammatory factors and reduce the neuroinflammatory response.³² In conclusion, the UPLC-LTQ-Orbitrap-MS technology was used in the present study to quickly and accurately identify the components of QFY into blood and brain, and preliminarily determine the basis of its pharmacodynamic substances.

The activation of microglia and the inflammatory phenotype are crucial for neuroprotection, but persistent microglial activation and neuroinflammation are the core pathological manifestations of some neurodegenerative diseases. In the early stage of AD, glial cells in the brain are more likely to be activated, and over-activated MG releases a large number of inflammatory factors, such as TNF- α , IL-1 β and complement. The activated microglia can be divided into the M1 and M2 types. M1 type cells mainly secrete proinflammatory factors, which have cytotoxic effects on neurons after long-term activation, while M2 type cells have the potentiality for phagocytosis, which can promote the growth of neurites.³³ Some studies have shown that long-term activation of M1 and inhibition of M2 are the basis of the inflammatory phenotype of AD and other chronic neurodegenerative diseases.³⁴ In the current study, QFY can reduce the expression of iNOS and CD16 mRNAs of M1 type markers, increase the expression of Arg-1 and IL-10 mRNAs of M2 type markers, and ultimately inhibit the expression of M1 type MG and reduce the occurrence of neuroinflammation.

The apoptosis of neurons affects the regeneration of neurons, which leads to the weakening of learning and memory abilities. The activation of the apoptosis pathway is mediated by the Caspase family of cysteine proteases, which cleave a variety of key cellular substrates.³⁵ At the same time, cell survival and apoptosis in mammals are also regulated by the Bcl-2 protein family. Our study found that QFY could reduce cell apoptosis and improve the memory abilities of AD mice by reducing the expression of Bax and caspase-1 proteins and increasing the expression of Bcl-2 protein, which was consistent with the results predicted by network pharmacology.

Overexpression of the M2 type of MG can activate intercellular adhesion factors, thus causing behavioral and cognitive impairment. Among them, ICAM-1 and MCP-1 can promote the recruitment, infiltration and activation of inflammatory cells, which are important mediators of the inflammatory reaction and are produced in large quantities at the site of tissue injury. TNF- α can cause the release of ICAM-1 and MCP-1 located in vascular endothelial cells, and then make relevant inflammatory factors enter the brain through the blood brain barrier to generate an inflammatory reaction.³⁴ In the current

experiment, we found that QFY could reduce the expression of ICAM-1 and MCP-1, and decrease the occurrence of inflammation. The occurrence of neuroinflammation will cause neuron loss, synaptic changes and dendrite reduction, and affect synaptic plasticity. Synaptic plasticity is considered to be the basis of brain learning and memory, which can complete signal transmission between neurons through its complex structure and diverse regulatory mechanisms. And, synaptic plasticity is closely related to the synaptic structure and function, which mediates the conduction of nerve excitability, and its impairment can lead to memory disorders and cognitive decline.³⁶ The overexpression of iNOS, the M1 type MG marker, increases NO synthesis, accelerates the toxic effect on nerve cells, causes the loss of dendritic spines, and then leads to synaptic damage.³⁷ As markers of synaptic plasticity, PSD95 and SYP can be observed in the early stages of AD patients.³⁸ Enhancing the expression of SYP and PSD95 in the hippocampus of AD mice can improve cognitive dysfunction.³⁹ In this study, we found that QFY dramatically increased the expression of PSD95 and SYP at the protein and mRNA levels, indicating that QFY had a protective effect on the function and structural damage of synapses in the hippocampus of D-gal model mice, and ultimately improved the cognitive function of the mice. Therefore, these results showed that regulating microglia phenotype and improving neuroinflammation might be one of the underlying molecular mechanisms of the anti-AD effect of QFY, as shown in Figure 8.

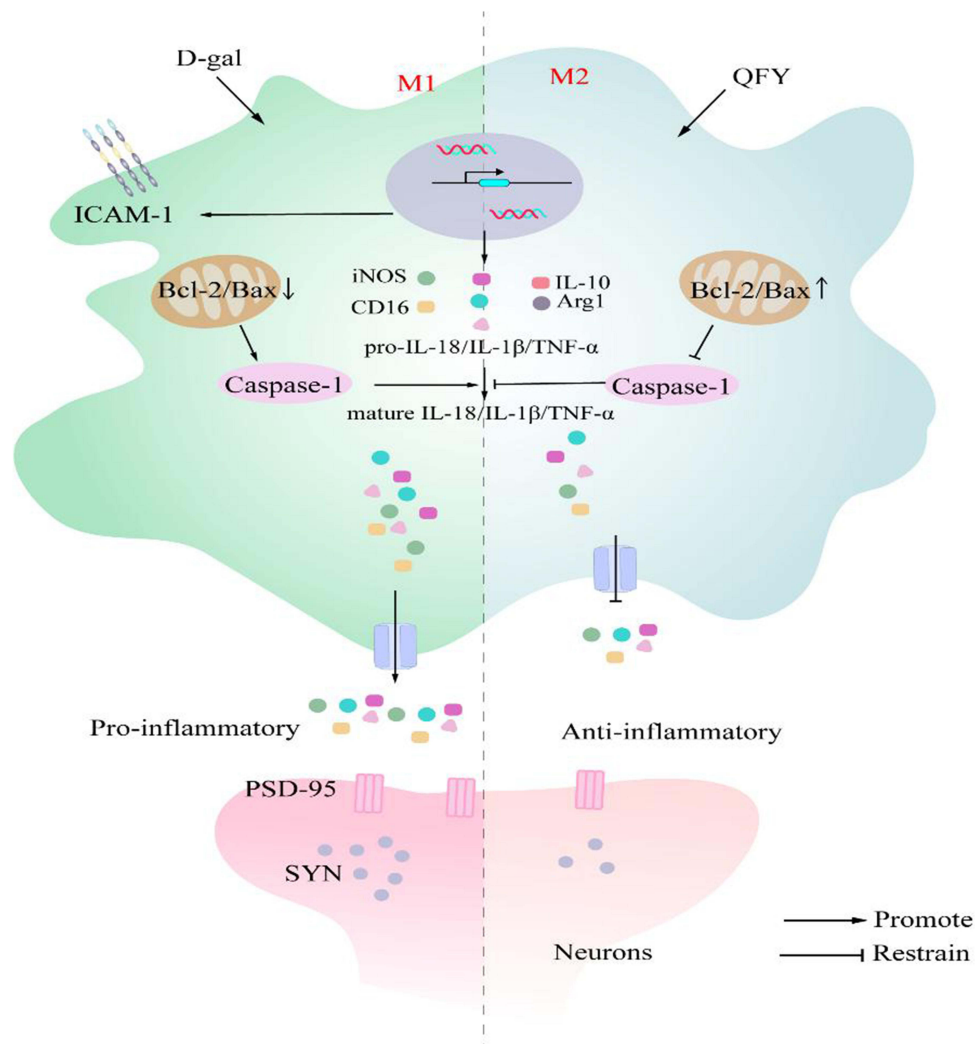


Figure 8 Diagram of the underlying mechanism of QFY in AD treatment.

Conclusion

After oral administration of QFY, 51 prototype components were absorbed in the blood and 15 prototype components were absorbed in the cerebrospinal fluid of mice, respectively. Many of these ingredients have anti-inflammatory and neuroprotective effects. Mechanistically, QFY could effectively improve the learning and memory impairment of D-gal-induced AD mice by inhibiting the excessive activation of microglia, enhancing the expression of M2 microglia, inhibiting the increase of inflammatory factors, cell adhesion factors and chemokines, anti-apoptosis, and improving synaptic plasticity. However, the biological activities and metabolic pathways of these components entering the blood, especially the brain, will be further investigated, and the pharmacokinetic analysis in blood and cerebrospinal fluid will be monitored to clarify the specific dose-effect relationship, which will provide experimental basis for better elucidating the pharmacodynamic substances and mechanisms of QFY in the treatment of AD in vivo.

Abbreviations

AD, Alzheimer's disease; CNS, Central nervous system; QFY, Qi-Fu-Yin; TCM, Traditional Chinese medicine; NOR, New object recognition; MWM, Morris water maze test; TEM, Transmission electron microscopy; MG, Morphology of microglia; SD, Sprague-Dawley; TCMSP, Traditional Chinese Medicine Systems Pharmacology; PPI, Protein-protein interaction; ELISA, Enzyme-linked immunosorbent assay; HE, Hematoxylin-eosin.

Data Sharing Statement

The data underlying this study is available from the corresponding author (X.L. Li, lixiaoli-ang-1984@163.com) on reasonable request.

Funding

This study was supported by the Hainan Provincial Natural Science Foundation of China (819MS061); National Natural Science Foundation of China (General Program, No. 81673581, 82174007); Heilongjiang Province Natural Science Foundation (No. LH2020H097); Talent Training Project Supported by the Central Government for the Reform and Development of Local Colleges and Universities; Scientific Research Project of the Wuxi Health Commission (M202206).

Disclosure

The authors report no conflicts of interest in this work.

References

1. Xu W, Jiang Y, Wang N, et al. Traditional Chinese Medicine as a promising strategy for the treatment of Alzheimer's disease complicated with osteoporosis. *Front Pharmacol.* 2022;13:1–18. doi:10.3389/fphar.2022.842101
2. Peng S, Li F, Yu K, et al. Integrating transcriptome and chemical analyses to reveal the anti-Alzheimer's disease components in *Verbena officinalis* Linn. *Front Plant Sci.* 2022;13:955075. doi:10.3389/fpls.2022.955075
3. Scheltens P, De Strooper B, Kivipelto M, et al. Alzheimer's disease. *Lancet.* 2021;397(10284):1577–1590. doi:10.1016/s0140-6736(20)32205-4
4. Kang N, Luan Y, Jiang Y, et al. Neuroprotective effects of oligosaccharides in *rehmannia* radix on transgenic *caenorhabditis elegans* Models for Alzheimer's disease. *Front Pharmacol.* 2022;13:878631. doi:10.3389/fphar.2022.878631
5. Yi P, Zhang Z, Huang S, Huang J, Peng W, Yang J. Integrated meta-analysis, network pharmacology, and molecular docking to investigate the efficacy and potential pharmacological mechanism of Kai-Xin-San on Alzheimer's disease. *Pharm Biol.* 2020;58(1):932–943. doi:10.1080/13880209.2020.1817103
6. Xiong W, Zhao X, Xu Q, et al. Qisheng Wan formula ameliorates cognitive impairment of Alzheimer's disease rat via inflammation inhibition and intestinal microbiota regulation. *J Ethnopharmacol.* 2022;282:114598. doi:10.1016/j.jep.2021.114598
7. Liu H, Zhong L, Dai Q, et al. Zuoguiwan ameliorates cognitive deficits and neuro-inflammation in streptozotocin-induced Alzheimer's disease rats. *Neuroimmunomodulation.* 2022;29(1):63–69. doi:10.1159/000516396
8. Xiao Q-Y, Ye T-Y, Wang X-L, et al. A network pharmacology-based study on key pharmacological pathways and targets of Qi Fu Yin acting on Alzheimer's disease. *Exp Gerontol.* 2021;149:111336. doi:10.1016/j.exger.2021.111336
9. Wang L, Qiao P, Yue L, Sun R. Is Qi Fu Yin effective in clinical treatment of dementia? A meta-analysis of 697 patients. *Medicine.* 2021;100(5):e24526. doi:10.1097/MD.00000000000024526
10. Ong WY, Wu YJ, Farooqui T, Farooqui AA. Qi Fu Yin-a Ming dynasty prescription for the treatment of dementia. *Mol Neurobiol.* 2018;55(9):7389–7400. doi:10.1007/s12035-018-0908-0

11. Li H, Zhao H, Yang Y, Qi D, Cheng X, Wang J. Identification of chemical components of Qi-Fu-Yin and its prototype components and metabolites in rat plasma and cerebrospinal fluid via UPLC-Q-TOF-MS. *Evid Based Complement Alternat Med.* 2021;2021:1995766. doi:10.1155/2021/1995766
12. Duan X, Li Y, Xu F, Ding H. Study on the neuroprotective effects of Genistein on Alzheimer's disease. *Brain Behav.* 2021;11(5):e02100. doi:10.1002/brb3.2100
13. Yu N, Huang Y, Jiang Y, et al. Ganoderma lucidum Triterpenoids (GLTs) reduce neuronal apoptosis via inhibition of ROCK signal pathway in APP/PS1 transgenic Alzheimer's disease mice. *Oxid Med Cell Longev.* 2020;2020:9894037. doi:10.1155/2020/9894037
14. Chuang Y, Van I, Zhao Y, Xu Y. Icariin ameliorate Alzheimer's disease by influencing SIRT1 and inhibiting A β cascade pathogenesis. *J Chem Neuroanat.* 2021;117:102014. doi:10.1016/j.jchemneu.2021.102014
15. R H. Alzheimer's disease. *Nature.* 2018;559(7715):1. doi:10.1038/d41586-018-05717-6
16. Chen Y, Dai Y, Xia J, et al. Serum pharmacochimistry combining network pharmacology to discover the active constituents and effect of Xijiao Dihuang Tang Prescription for treatment of blood-heat and blood-stasis syndrome-related disease. *Oxid Med Cell Longev.* 2022;2022:6934812. doi:10.1155/2022/6934812
17. Wei J, Yu Y, Zhang Y, et al. Integrated serum pharmacochimistry and network pharmacology approach to explore the effective components and potential mechanisms of menisperm rhizoma against myocardial ischemia. *Front Chem.* 2022;10:869972. doi:10.3389/fchem.2022.869972
18. Ma FX, Xue PF, Wang YY, Wang YN, Xue SY. Research progress of serum pharmacochimistry of traditional Chinese medicine. *Zhongguo Zhong Yao Za Zhi.* 2017;42(7):1265–1270. doi:10.19540/j.cnki.cjcm.20170224.010
19. Jiang N, Wei S, Zhang Y, et al. Protective effects and mechanism of radix polygalae against neurological diseases as well as effective substance. *Front Psychiatry.* 2021;12:688703. doi:10.3389/fpsy.2021.688703
20. Wang H, Huang H, Jiang N, Zhang Y, Lv J, Liu X. Tenuifolin ameliorates chronic restraint stress-induced cognitive impairment in C57BL/6J mice. *Phytother Res.* 2022;36(3):1402–1412. doi:10.1002/ptr.7402
21. Lee HK, Yang EJ, Kim JY, Song KS, Seong YH. Inhibitory effects of Glycyrrhizae radix and its active component, isoliquiritigenin, on A β (25–35)-induced neurotoxicity in cultured rat cortical neurons. *Arch Pharm Res.* 2012;35(5):897–904. doi:10.1007/s12272-012-0515-y
22. Sun YX, Tang Y, Wu AL, et al. Neuroprotective effect of liquiritin against focal cerebral ischemia/reperfusion in mice via its antioxidant and antiapoptosis properties. *J Asian Nat Prod Res.* 2010;12(12):1051–1060. doi:10.1080/10286020.2010.535520
23. Zhang Y, Qiao L, Song M, Wang L, Xie J, Feng H. Hplc-ESI-MS/MS analysis of the water-soluble extract from Ziziphi spinosae semen and its ameliorating effect of learning and memory performance in mice. *Pharmacogn Mag.* 2014;10(40):509–516. doi:10.4103/0973-1296.141777
24. Thapliyal S, Singh T, Handu S, et al. A Review on Potential Footprints of Ferulic Acid for Treatment of Neurological Disorders. *Neurochem Res.* 2021;46(5):1043–1057. doi:10.1007/s11064-021-03257-6
25. Yim NH, Gu MJ, Park HR, Hwang YH, Ma JY. Enhancement of neuroprotective activity of Sagunja-tang by fermentation with lactobacillus strains. *BMC Complement Altern Med.* 2018;18(1):312. doi:10.1186/s12906-018-2361-z
26. Wang X, Wu C, Xu M, Cheng C, Liu Y, Di X. Optimisation for simultaneous determination of iridoid glycosides and oligosaccharides in Radix Rehmannia by microwave assisted extraction and HILIC-UHPLC-TQ-MS/MS. *Phytochem Anal.* 2020;31(3):340–348. doi:10.1002/pca.2900
27. Zhang L, Dai W, Zhang X, Gong Z, Jin G. Mannotriose regulates learning and memory signal transduction in the hippocampus. *Neural Regen Res.* 2013;8(32):3020–3026. doi:10.3969/j.issn.1673-5374.2013.32.005
28. Ardah MT, Paleologou KE, Lv G, et al. Ginsenoside Rb1 inhibits fibrillation and toxicity of alpha-synuclein and disaggregates preformed fibrils. *Neurobiol Dis.* 2015;74:89–101. doi:10.1016/j.nbd.2014.11.007
29. Ye R, Kong X, Yang Q, Zhang Y, Han J, Zhao G. Ginsenoside Rd attenuates redox imbalance and improves stroke outcome after focal cerebral ischemia in aged mice. *Neuropharmacology.* 2011;61(4):815–824. doi:10.1016/j.neuropharm.2011.05.029
30. Munteanu IG, Apetrei C. A review on electrochemical sensors and biosensors used in chlorogenic acid electroanalysis. *Int J Mol Sci.* 2021;22(23):13138. doi:10.3390/ijms222313138
31. Szliszka E, Czuba ZP, Domino M, Mazur B, Zydowicz G, Krol W. Ethanol extract of propolis (EEP) enhances the apoptosis-inducing potential of TRAIL in cancer cells. *Molecules.* 2009;14(2):738–754. doi:10.3390/molecules
32. Zhou Z, Hou J, Mo Y, et al. Geniposidic acid ameliorates spatial learning and memory deficits and alleviates neuroinflammation via inhibiting HMGB-1 and downregulating TLR4/2 signaling pathway in APP/PS1 mice. *Eur J Pharmacol.* 2020;869:172857. doi:10.1016/j.ejphar.2019.172857
33. Yang YH, Zhu J. Targeting miR-106-3p facilitates functional recovery via inactivating inflammatory microglia and interfering glial scar component deposition after neural injury. *Eur Rev Med Pharmacol Sci.* 2019;23:9001–9008.
34. Sun X, Gao J, Meng X, Lu X, Zhang L, Chen R. Polarized macrophages in periodontitis: characteristics, function, and molecular signaling. *Front Immunol.* 2021;12:763334. doi:10.3389/fimmu.2021.763334
35. Hansen E, Krautwald M, Maczurek AE, et al. A versatile high throughput screening system for the simultaneous identification of anti-inflammatory and neuroprotective compounds. *J Alzheimers Dis.* 2010;19(2):451–464. doi:10.3233/JAD-2010-1233
36. Cornell J, Salinas S, Huang HY, Zhou M. Microglia regulation of synaptic plasticity and learning and memory. *Neural Regen Res.* 2022;17(4):705–716. doi:10.4103/1673-5374.322423
37. Takamori M. Myasthenia gravis: from the viewpoint of pathogenicity focusing on acetylcholine receptor clustering, trans-synaptic homeostasis and synaptic stability. *Front Mol Neurosci.* 2020;13:86. doi:10.3389/fnmol.2020.00086
38. Dinda B, Dinda M, Kulsi G, Chakraborty A, Dinda S. Therapeutic potentials of plant iridoids in Alzheimer's and Parkinson's diseases: a review. *Eur J Med Chem.* 2019;169:185–199. doi:10.1016/j.ejmech.2019.03.009
39. Liu J, Liu B, Yuan P, et al. Role of PKA/CREB/BDNF signaling in PM2.5-induced neurodevelopmental damage to the hippocampal neurons of rats. *Ecotoxicol Environ Saf.* 2021;214:112005. doi:10.1016/j.ecoenv.2021.112005

Drug Design, Development and Therapy

Dovepress

Publish your work in this journal

Drug Design, Development and Therapy is an international, peer-reviewed open-access journal that spans the spectrum of drug design and development through to clinical applications. Clinical outcomes, patient safety, and programs for the development and effective, safe, and sustained use of medicines are a feature of the journal, which has also been accepted for indexing on PubMed Central. The manuscript management system is completely online and includes a very quick and fair peer-review system, which is all easy to use. Visit <http://www.dovepress.com/testimonials.php> to read real quotes from published authors.

Submit your manuscript here: <https://www.dovepress.com/drug-design-development-and-therapy-journal>